Published in "Journal of Magnetism and Magnetic Materials 396:
345–349, 2015"
which should be cited to refer to this work.

Magnetic exchange interactions in Mn doped $ZnSnAs_2$ chalcopyrite

H. Bouhani-Benziane [a], O. Sahnoun [a], M. Sahnoun [a,c,*], M. Driz [b], C. Daul [c]

[a] Laboratoire de Physique Quantique de la Matière et Modélisation Mathématique (LPQ3M), University of Mascara, Algeria
[b] Laboratoire de Sciences des Matériaux (LSM), University of Sidi Bel Abbes, Algeria
[c] Department of Chemistry, University of Fribourg, Switzerland

Accurate ab initio full-potential augmented plane wave (FP-LAPW) electronic calculations within generalized gradient approximation have been performed for Mn doped $ZnSnAs_2$ chalcopyrites, focusing on their electronic and magnetic properties as a function of the geometry related to low Mn-impurity concentration and the spin magnetic alignment (i.e., ferromagnetic vs antiferromagnetic). As expected, Mn is found to be a source of holes and localized magnetic moments of about 4 μ_B per Mn atom are calculated which are sufficiently large. The defect calculations are firstly performed by replacing a single cation (namely Zn and Sn) with a single Mn atom in the pure chalcopyrite $ZnSnAs_2$ supercell, and their corresponding formation energies show that the substitution of a Sn atom (rather than Zn) by Mn is strongly favored. Thereafter, a comparison of total energy differences between ferromagnetic (FM) and antiferromagnetic (AFM) are given. Surprisingly, the exchange interaction between a Mn pairs is found to oscillate with the distance between them. Consequently, the AFM alignment is energetically favored in Mn-doped $ZnSnAs_2$ compounds, except for low impurity concentration associated with lower distances between neighboring Mn impurities, in this case the stabilization of FM increases. Moreover, the ferromagnetic alignment in the Mn-doped $ZnSnAs_2$ systems behaves half-metallic; the valence band for majority spin orientation is partially filled while there is a gap in the density of states for the minority spin orientation. This semiconducting gap of $\sim$1 eV opened up in the minority channel and is due to the large bonding–antibonding splitting from the p–d hybridization. Our findings suggest that the Mn-doped $ZnSnAs_2$ chalcopyrites could be a different class of ferromagnetic semiconductors.

1. Introduction

Half-metallic antiferromagnets (HM-AFM) with a small value of the total magnetic moment are much more desirable in magnetoelectronics applications, in the sense that the majority spin and minority spin densities of states are not identical, and having a magnetic moment that is, due to the half-metallic character, precisely equal to zero. Such system would be a very interesting magnetoelectronics material since it would be a perfectly stable spin-polarized electrode in a junction device [1]. And moreover if used as a tip in a spin-polarized STM, it would not give rise to stray flux, and hence would not distort the domain structure of the soft-magnetic systems to be studied [2]. The first concept for HM-AFM was proposed by van Leuken and de Groot in 1995 [3] in their pioneer work on half-metallic magnets. Since the initial theoretical predictions of HM-AFM in Heusler alloys [4], several candidates have been reported in double perovskites [5–8]. Despite several experimental challenges [9] no actual HM-AFMs have been synthesized yet.

Quite recently, high-temperature ferromagnetism was found to exist in chalcopyrite-type compounds by introducing ferromagnetic (FM) property at room temperature via doping them by transition materials (TM) impurities. Among them manganese-doped II–IV–V_2 chalcopyrite's such as $ZnGeP_2$:Mn [10], $CdGeP_2$:Mn [11], $ZnGeAs_2$:Mn, $ZnSiAs_2$:Mn, $CdGeAs_2$:Mn [12] and $ZnSnAs_2$:Mn [13] have demonstrated Curie temperatures of up to 367 K. The general consensus among researchers in this area is that ferromagnetism in these materials originates from the interactions between itinerant electrons or holes and localized electrons. In this context Choi et al. [13] reported experimentally the discovery of ferromagnetism in Mn-doped $ZnSnAs_2$ single crystal with Curie temperature of 329 K. They found that the magnetic moment from saturation magnetization per Mn atom is around 3.63 μ_B at 5 K. However, from theoretical point of view, Yi et al. [14] point out that $ZnSn_{1-x}Mn_xAs_2$ for $x=0.125$ prefers the AFM ground state rather than the FM state. In addition, the local structures around Mn atoms in the $ZnSnAs_2$:Mn studied by XAFS measurements

* Corresponding author.
E-mail address: sahnoun_cum@yahoo.fr (M. Sahnoun).

demonstrated that the Mn atoms are substituted into both Zn and Sn cation sites [15]. However, the physical origin of FM or AFM states in Mn-doped II–IV–V_2 chalcopyrites is still in debate [16,17] and more theoretical and experimental studies are required. This situation motivates us to study the electronic and magnetic properties of Mn-doped $ZnSnAs_2$ chalcopyrite, using the full potential linearized augmented plan wave plus orbital's local (FP-LAPW+*lo*), in order to give more understand about the properties of herein materials. In the following discussions, the possible HM-AFM states are highlighted.

2. Methods of calculation

All calculations presented in the present work were performed using the full potential linearized augmented plane-wave (LAPW) method as implemented in the *Wien2k* package [18]. The electronic exchange–correlation is described within the generalized gradient approximation (GGA) of Perdew–Burke–Ernzerhof (PBE) [19]. The wave function of the charge density and potential in the interstitial region is expanded up to $l_{max}=10$, as well as the energy cut-off of $R_{MT}\cdot K_{max}=7.0$ were kept fixed in our calculation, where R_{MT} denotes the smallest atomic sphere radius and K_{max} gives the magnitude of the largest K vector in the plane wave expansion. In order to simulate magnetic properties we have modeled the situation when manganese atoms replace either the site of Zn (Mn_{Zn}) or the site of Sn (Mn_{Sn}) atoms. The Mn doping has been modeled in a sufficiently large and fully relaxed supercell, which is a $2\times2\times1$ translated 64-atoms simple tetragonal.

3. Results and discussion

3.1. Electronic structures of the $ZnSnAs_2$ chalcopyrite

In order to compute the density of states of $ZnSnAs_2$ having the chalcopyrite structure, we first determine the lattice parameters. $ZnSnAs_2$ compound crystallizes in the chalcopyrite structure with space group no. 122 (I-42d) having four formula units in each unit cell which is shown in Fig. 1. The chalcopyrite unit cells are a body-centered tetragonal distorted unit cell, and the c/a ratio may differ from ideal value of 2. This structure has two cations Zn and Sn atoms which are tetrahedrally bonded to As anions. Atomic sites for $ZnSnAs_2$ are Zn(0.0,0.0,0.0), Sn(0.0,0.0,0.5), and As (u,0.25,0.125), where u is the internal distortion parameter. The calculation of the total energy as a function of the volume was used for determination of theoretical lattice constant and bulk modulus of the compound. The equilibrium lattice constant, bulk modulus, and its pressure derivative are calculated by fitting the calculated total energy into the Murnaghan's equation of state. The calculated lattice parameters of $ZnSnAs_2$ are $a=5.942$ Å, $c=11.957$ Å, and $u=0.225$. The lattice parameters a and c are consistent with the experimental results of $a=5.908$ Å and $c=11.670$ Å [20]. The calculated u parameter is the same to the experimental value [21]. Indeed taking the equilibrium positions, we compute the electronic structure of the $ZnSnAs_2$ chalcopyrite. It reveals that the total density of states (DOS) of $ZnSnAs_2$ as well as the partial DOS related to Zn (3d), Sn (5s,5p) and As (4p) are in accordance with previous theoretical calculations [22]. It follows from Fig. 2 that the valence band (VB) of $ZnSnAs_2$ is composed mainly of the partial states As(4p) and Sn(5p). The conduction band (CB) is composed of the As(4p) and Sn(5s) states. The Zn(3d) states mainly appear in the narrow energy range of -7.5 to 5.5 eV. There is a strong hybridization between Zn(3d)–As(4p) and Sn (5p)–As(4p) states, indicating obviously covalent character. The obtained band gap is about 0.60 eV, which is in reasonable accord compared with the experimental value of 0.65 eV [13].

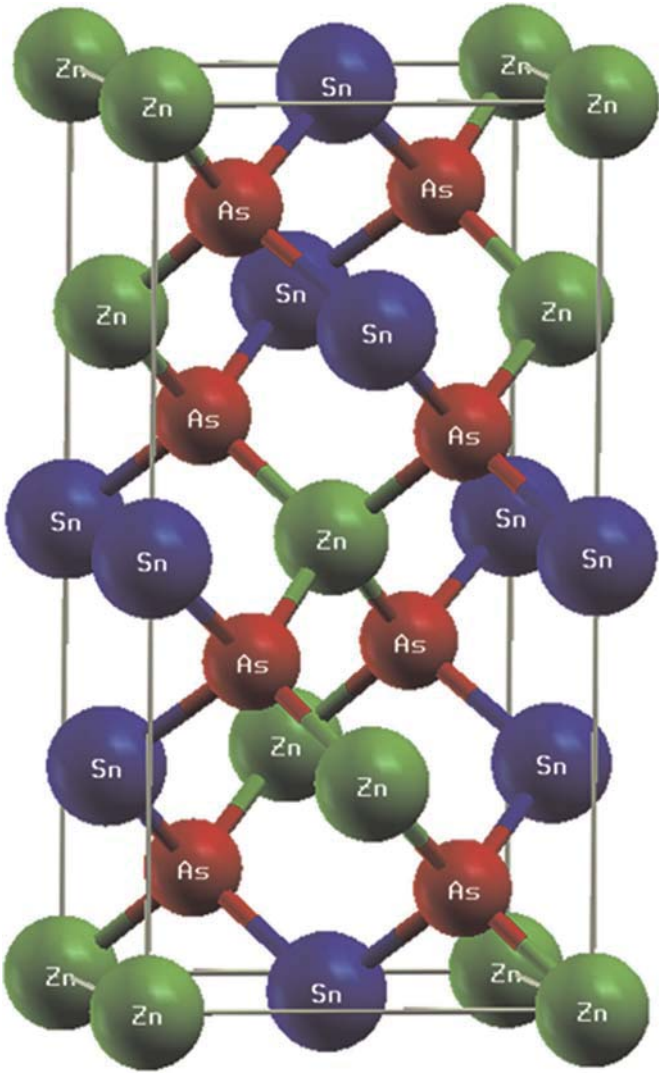

Fig. 1. Unit cell of $ZnSnAs_2$ chalcopyrite structure.

3.2. Magnetic properties in the Mn-doped $ZnSnAs_2$ chalcopyrite

The defect calculations are performed by placing a single Mn atom in a supercell, containing 64 atoms and having lattice vectors (2,0,0)a, (0,2,0)a, and (0,0,ηu)a; the lattice parameters a and $c=2a\eta u$ are chosen as for the pure bulk chalcopyrite. In this case, the systems are in a ferromagnetic configuration. We consider substitutional defects, i.e., replacing a single cation (namely Zn and Sn) with a Mn atom in the pure chalcopyrite $ZnSnAs_2$ cell. The formation energy of a defect is estimated as follows [23]:

$$E_f=\frac{1}{64}[E((\mathrm{Zn,\ Sn})_{1-x}\mathrm{Mn_xAs_2})-E(\mathrm{ZnSnAs_2})-\mu(\mathrm{Mn})+\mu(\mathrm{Zn,\ Sn})]$$

where $E((Zn,Sn)_{1-x}Mn_xAs_2)$ is the total energy of the supercell containing the Mn dopant, $E(ZnSnAs_2)$ is the total energy of the pure host having the same dimension to supercell, and μ_{Mn} and $\mu_{(Zn,Sn)}$ are the chemical potentials of bulk Mn, Zn and Sn, respectively. Our calculated formation energies of a Mn defect in $ZnSnAs_2$ are 0.248 eV and 0.216 eV for Mn substituting Zn and Sn, respectively. In the chosen limit of the chemical potentials, this implies that the substitution of a Sn atom (rather than Zn) by Mn is strongly favored.

Generally, when 3d TM ions are substituted for the cations of

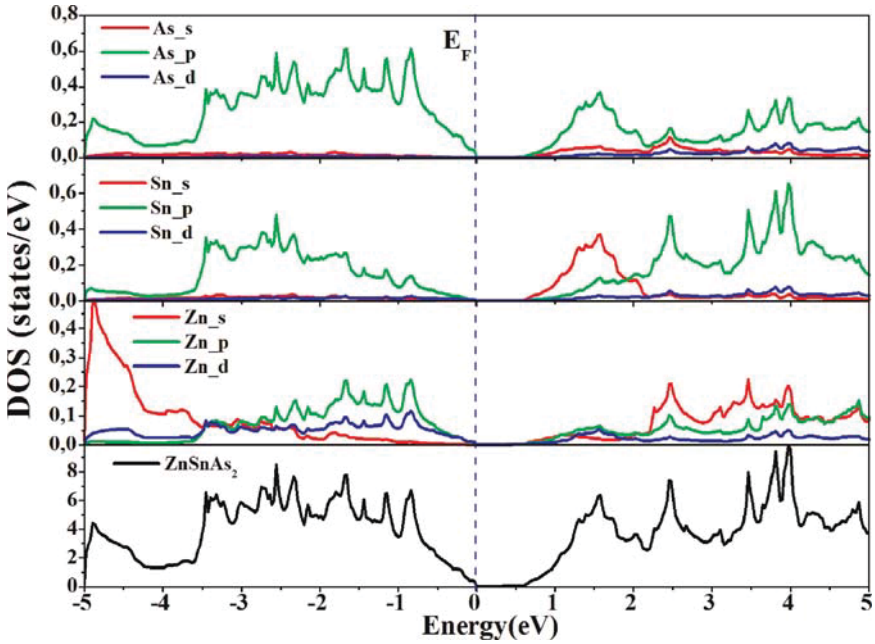

Fig. 2. Total and partial DOS of $ZnSnAs_2$.

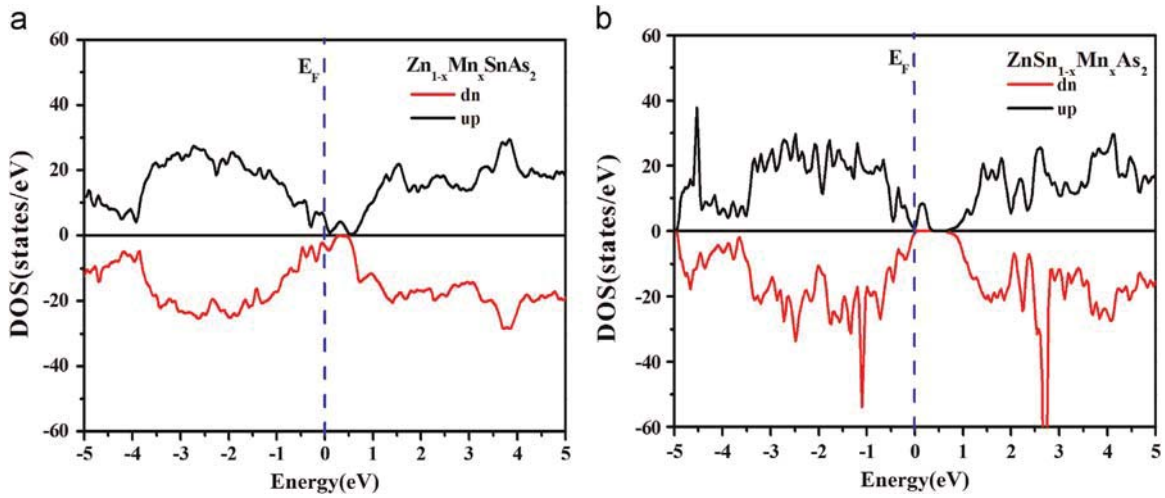

Fig. 3. Total density of states for Mn doped $ZnSnAs_2$. Only a single Mn atom is substituted into Zn or Sn cation sites in the supercell of 64 atoms (x=0.0625).

the host, their electronic structure is influenced by the strong 3d orbitals of the magnetic ion and the p orbitals of the neighboring anions. In our case, the hybridization between Mn dopant and its neighboring host atoms results in the splitting of the energy levels near the E_F, which shifts the majority spin states downward and minority spin states upward. Density of states in Fig. 3 show spin splitting between the majority-spin and minority-spin channel near E_F, which implies that Mn doping can result in magnetism in the $ZnSnAs_2$ host. When Mn ions substitute on Zn and Sn sites, the obtained magnetic moment per Mn is 4.00 μ_B and 3.90 μ_B, respectively, which is in reasonable agreement with the experimental moment (3.85 μ_B/Mn) for Mn-doped $ZnSnAs_2$ (x=0.056) [8] assumed due to substitution on both Zn and Sn sites.

3.3. Electronic structure of the $ZnSn_{0.875}Mn_{0.125}As_2$ doped chalcopyrite

This part will be devoted to understand and to clarify the mechanism which stabilizes the ferromagnetic states in the $ZnSn_{0.875}Mn_{0.125}As_2$ doped chalcopyrite. To do so, we first calculate the density of states (DOS) of this system in the GGA approximation. The magnetic moments localized on substitutional Mn ions in $ZnSnAs_2$ chalcopyrite may interact not only with delocalized valence and conduction band carriers. They, of course, may also interact between each other either indirectly or directly. All the collective magnetic phenomena are caused by interactions between those microscopic magnetic moments. The most important of these interactions is the exchange interaction. It is purely electrostatic by nature and can have several underlying mechanisms.

In order to understand the variation of exchange interaction, the concentration of Mn atoms was put to 12.5%, equivalent to introducing 2 Mn atoms in the same supercell but with different geometries. Our results are presented in Fig. 4. It follows for this figure that the Mn(3d) orbitals are no longer located in the gap, but widely hybridized in the valence band. This does not exclude the effect of the strong correlation but their influence on the density of states is much less visible.

The interaction of Mn with the As-p states splits the Mn-3d states into a low-lying doublet of e states ($d_{3z^2-r^2}$ and $d_{x^2-y^2}$) and a

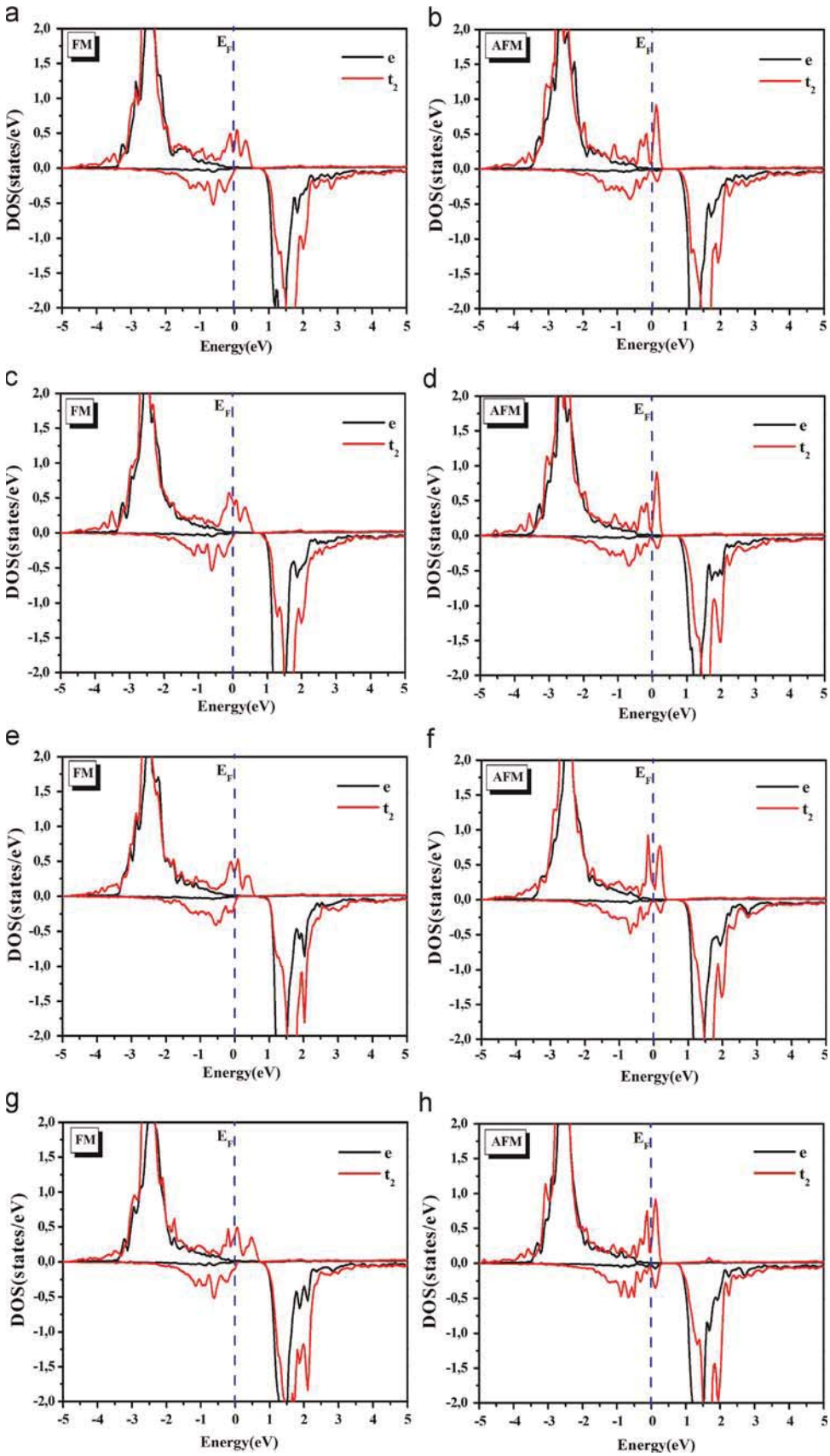

Fig. 4. Mn-d projected density of states for the FM and AFM $ZnSn_{0.875}Mn_{0.125}As_2$ for different distances between Mn pairs. (a,b) $d=7.307$ Å, (c,d) $d=7.284$ Å, (e,f) $d=5.941$ Å, and (g,h) $d=4.214$ Å.

Table 1
The calculated results for distances defining various Mn pairs configurations into the $Zn_{16}Sn_{14}Mn_2As_{32}$ supercell. ΔE is the FM stabilization energy between the AFM and FM states and their corresponding magnetic moment at each Mn atom.

Distance Mn–Mn (Å)	ΔE (mRy)	μ_{Mn} (FM) (μ_B)	μ_{Mn} (AFM) (μ_B)
4.214	−8.996	3.92739	4.00078
5.941	1.645	3.98550	4.00370
7.284	1.898	4.00305	4.01791
7.307	2.071	3.93192	4.01425

higher-lying triplet of t_2 states (d_{xy}, d_{yz} and d_{xz}). The splitting is partly due to the different electrostatic repulsion, which is strongest for the e states which directly point at the As atoms. In the minority band the Mn(3d) states are shifted to lower energies and form a common 3d band with the other Mn(3d) states, while in the majority band the Mn-3d states are shifted to higher energies and are partially unoccupied, so that a band gap at E_F is formed, separating the occupied d bonding states from the unoccupied d antibonding states (see Fig. 4). Thus $ZnSn_{0.875}Mn_{0.125}As_2$ is a half-metal with a gap at E_F in majority band and a metallic DOS at the Fermi level in minority band. The presence of an extra Mn atom in the chalcopyrite structure makes the interactions more complex. The important interactions arise between nearest Mn atoms (Mn–Mn interactions) and are responsible for the stability of the ferromagnetism in the $ZnSn_{0.875}Mn_{0.125}As_2$ doped chalcopyrite.

Table 1 shows that for all different geometries, relative to the distances between the Mn impurities, there have nonzero magnetic moments. This observation drives us to determine the most stable magnetic state for such systems. In order to reach that, the magnetic energy difference (ΔE) between the ferromagnetic state (FM) and the antiferromagnetic state (AFM) has been calculated. It is known that this quantity determines the stabilization of the magnetic phase in the diluted magnetic semiconductors (DMS). In particular, the negative value of this quantity corresponds to the fact that the AFM state is more stable than FM state and vise versa. The complete calculation of the variation of the ΔE as function of our $ZnSn_{0.875}Mn_{0.125}As_2$ doped systems with different geometries is then presented (Table 1). It follows that the antiferromagnetic state is more stable than the ferromagnetic state for Mn–Mn neighboring distances corresponding to the values higher than 4.21 Å. The ferromagnetic Mn–Mn interactions are mainly responsible for the stable ferromagnetism of these materials. At the larger distance between neighboring Mn atoms the leading Mn–Mn interaction is negative resulting in the antiferromagnetic behavior of the system. On the other hand, for the contracted distances the interaction changes sign resulting in the ferromagnetic ground state of the alloy. This complexity of the behavior reflects the complexity of the electronic structure of the systems.

4. Conclusion

Using the first-principles density functional theory within the GGA, we have studied the electronic structure of $ZnSnAs_2$ doped with 12.5% Mn impurities for various possible geometries to replicate the situation where the Mn atom would appear either to cluster or be separated. The calculated total magnetic moment is about 4 μ_B per unit cell and mostly located in Mn atom. Our results show that the substitution of Mn leads to the AFM alignment is energetically favored in Mn-doped $ZnSnAs_2$ compounds; except for low impurity concentration associated with lower distances between Mn pairs, in this case the stabilization of FM increases. Moreover, the ferromagnetic alignment in the Mn-doped $ZnSnAs_2$ systems behaves half-metallic; the valence band for majority spin orientation is partially filled while there is a gap in the density of states for the minority spin orientation.

Acknowledgment

This work was supported by the National Research Program of Algeria CNEPRU under Grant no. D03720130023.

References

[1] W.E. Pickett, Phys. Rev. Lett. 77 (1996) 3185.
[2] K. Özdogan, I. Galanakis, E. Şaşioglu, B. Aktaş, J. Phys.: Condens. Matter 18 (2006) 2905.
[3] H. van Leuken, R.A. de Groot, Phys. Rev. Lett. 74 (1995) 1171.
[4] I. Galanakis, K. Özdöğan, E. Şaşoğlu, B. Aktaş, Phys. Rev. B 75 (2007) 092407.
[5] J.H. Park, S.K. Kwon, B.I. Min, Phys. Rev. B 65 (2002) 174401.
[6] W. Song, J. Wang, Z. Wu, Chem. Phys. Lett. 501 (2011) 324.
[7] S.H. Chen, Z.R. Xiao, Y.P. Liu, Y.K. Wang, J. Appl. Phys. 108 (2010) 093908.
[8] C.Q. Tang, Y. Zhang, J. Dai, Solid State Commun. 133 (2005) 219.
[9] M. Nakao, Phys. Rev. B 74 (2006) 172404.
[10] G.A. Medvedkin, K. Hirose, T. Ishibashi, T. Nishi, V.G. Voevodin, K. Sato, J. Cryst. Growth 609 (2002) 236.
[11] G.A. Medvedkin, T. Ishibashi, T. Nishi, K. Hayata, Y. Hasegawa, K. Sato, Jpn. J. Appl. Phys. 10A (2000) L949.
[12] A.S. Morozov, L.A. Koroleva, D.M. Zashchirinskii, T.M. Khapaeva, S.F. Marenkin, I.V. Fedorchenko, R.A. Szymczak, B. Krzymanska, Solid State Phenom. 31 (2011) 168–169.
[13] S. Choi, G.B. Cha, S.C. Hong, S. Cho, Y. Kim, J.B. Ketterson, S.Y. Jeong, G.C. Yi, Solid State Commun. 122 (2002) 165.
[14] H. Yi, S. Lee, J. Magn. Magn. Mater. 272 (2004) e243.
[15] H. Oomae, H. Toyota, S. Emura, H. Asahi, N. Uchitomi, EPJ Web Conf. 75 (2014) 09004.
[16] A.J. Freeman, Y.-J. Zhao, J. Phys. Chem. Solids 64 (2003) 1453.
[17] Z. Yu-Jun, S. Picozzi, A. Continenza, W.T. Geng, A.J. Freeman, Phys. Rev. B 65 (2002) 094415.
[18] P. Blaha, K. Schwarz, G. Madsen, D. Kvasicka, J. Luitz, WIEN2K, An Augmented Plane Wave Local Orbitals Program for Calculating Crystal Properties, Technical University of Vienna, Vienna, 2001.
[19] K. Ozdogan, M. Upadhyay Kahaly, S.R. Sarath Kumar, H.N. Alshareef, U. Schwingenschlogl, J. Appl. Phys. 111 (2012) 054313.
[20] V.L. Shaposhnikov, A.V. Krivosheeva, V.E. Borisenko, Phys. Rev. B 85 (2012) 205201.
[21] A.A. Vaipolin, Sov. Phys. Solid State 15 (1973) 965.
[22] S. Mishra, B. Ganguli, J. Solid State Chem. 200 (2013) 279.
[23] C.-W. Zhang, S.-S. Yan, Appl. Phys. Lett. 95 (2009) 232108.